Decay of ^{101}Sr and the rotational structure of ^{101}Y

R. F. Petry and J. D. Goulden
University of Oklahoma, Norman, Oklahoma 73019

F. K. Wohn and John C. Hill
Ames Laboratory and Iowa State University, Ames, Iowa 50011

R. L. Gill and A. Piotrowski*
Brookhaven National Laboratory, Upton, New York 11973

(Received 24 August 1987)

The level structure of ^{101}Y has been studied through the β decay of ^{101}Sr. Ninety-six γ rays are placed in a level scheme with 34 levels. The first 14 levels of ^{101}Y (below 1.1 MeV) are identified as members of the four rotational bands associated with the Nilsson orbitals (with bandhead energies in keV) $\frac{5}{2}$[422] (0), $\frac{3}{2}$[301] (510), $\frac{5}{2}$[303] (666), and $\frac{1}{2}$[301] (890). Above 1.2 MeV occur six low-spin ($I \leq \frac{7}{2}$) levels that have features expected for members of $\frac{1}{2}$[431] and $\frac{3}{2}$[431] bands, but it is not possible to make unambiguous assignments of all six levels to these two bands. The level energies and γ-decay patterns (both intraband and interband) are well reproduced by simple particle-rotor calculations consisting of single quasiparticles coupled to an axially symmetric core. As is the case for ^{99}Y, the rotational structure of ^{101}Y indicates an axially symmetric deformation ϵ near the middle of the range of $0.3 < \epsilon < 0.4$. Similarities and differences between the bands observed in ^{99}Y and ^{101}Y are discussed and compared to model predictions.

I. INTRODUCTION

The characterization of transitional nuclei in the $A \sim 100$ region has received considerable attention in the past few years. Interest in this region has been stimulated by the development of new experimental facilities, particularly on-line mass separator facilities, which have permitted systematic studies of the level structures of several of these nuclides. The detailed results that have emerged from these studies have been given in a number of papers, and a rather complete list is contained in Ref. 1.

To summarize the conclusions of these studies, we note that the general character of the region appears to be very similar to that of the rare-earth region. There is a shape transition from spherical to prolate deformed for nuclei with $Z \leq 40$ as the neutron number increases from 58 to 60 [U(5) to SU(3) in IBA language], while for $Z \geq 44$ and the same neutron numbers the transition appears instead to involve axially asymmetric shapes [U(5) to O(6)]. The primary difference from the rare-earth region is that in terms of the usual indicators, which include the $E(2_1^+)$ and $E(4_1^+)/E(2_1^+)$ systematics in the even-even nuclei, the shape transition in the $A \sim 100$ region is much sharper. Furthermore, the prolate deformed $A \sim 100$ nuclei have moments of inertia ranging from 70% of the rigid-body value for even-even nuclei to more than 90% for odd-odd nuclei, values that are significantly larger than those observed in the rare-earth region.[2] The abruptness of the shape transition has been attributed to an unusually effective n-p interaction relative to p-p and n-n pairing correlations.[3] This effect is particularly strong in the $A \sim 100$ region because of the simultaneous filling of the proton $g_{9/2}$ and neutron $g_{7/2}$ spin-orbit partner orbitals as suggested by Federman and Pittel.[3] This effect, which appears to offer an explanation for shape transitions in general, is enhanced for $A \sim 100$ nuclei compared to rare-earth nuclei because of the presoftening of the effect in the rare-earth region due to intermediate spin (e.g., $\pi d_{5/2}$ and $\nu f_{7/2}$) orbitals. It should also be noted that in both odd-A and even-even nuclei in the $A \sim 100$ region there is strong evidence for excited states with a spherical basis in nuclei with large ground-state deformations. This coexistence of spherical and deformed shapes had been predicted in potential-energy-surface calculations.[4,5]

For the odd-A nuclides in the region with $N \geq 60$, a picture similar to that given by Bunker and Reich[6] for the rare-earth region is emerging. The level structure below ~ 1 MeV for a number of nuclei can be convincingly understood in terms of Nilsson states near the Fermi surface acting as bandheads upon which rotational structures are built. The structure of these one-quasiparticle rotational bands in deformed odd-A nuclei has been discussed in the framework of particle-rotor calculations in Refs. 7 and 8. Above ~ 1 MeV nonrotational states also may be understood, at least qualitatively, in terms of quasiparticle couplings to core vibrations or other three-quasiparticle states. Recently, the 8.6-μs isomer[9] in ^{99}Y (at 2142 keV and with $I^\pi = 17/2^+$) and a $K^\pi = 11/2^+$ rotational bandhead at 1655 keV have been described in terms of such three-quasiparticle configurations.[10]

In the following sections we present, for the first time, detailed experimental results for the decay of ^{101}Sr and our analysis of the level structure of ^{101}Y. Section II contains a description of the experimental methods and a listing of the results. In Sec. III we give a brief discussion

of the construction of the level scheme of ^{101}Y and describe the arguments used to make the band assignments. Finally, Sec. IV contains the results of particle-rotor calculations which further support the band assignments of Sec. III and a detailed comparison of the level structures of the isotopes ^{99}Y and ^{101}Y.

II. EXPERIMENTAL METHODS AND RESULTS

A. Source preparation

Mass-separated sources of ^{101}Sr were produced at the TRISTAN isotope separator facility operating on line to the high flux beam reactor at Brookhaven National Laboratory. Targets of ~ 5 g of ^{235}U situated in the separator's ion source were exposed to a neutron flux of $\sim 2\times 10^{10}/\text{cm}^2\text{s}$. Two different ion sources were used in two separate experiments. In the earlier experiment a positive surface ionization source with a Ta ionizer produced very weak beams of ^{101}Sr when operated at a very high temperature ($\sim 2300\,^{\circ}$C). There was no evidence of either primary ^{101}Rb or ^{101}Y in the beam, and we have assumed that the beam was pure ^{101}Sr. (A later check with a much higher yield Ta ionizer source also failed to produce any evidence for ^{101}Rb.) In the second experiment a similar ion source was used, but with a Re ionizer. Yields of ^{101}Sr were at least five times greater in this experiment because of the improved ionization efficiency for Sr. In neither experiment was there any evidence for cross contamination from adjacent masses. The ion sources used were modified versions of the ion sources described in Ref. 11.

B. Measurements

The same experimental configuration was used in both experiments. The mass-separated ion beam was collected on movable, aluminum-coated mylar tape. Because of the short half-life of ^{101}Sr, the source was viewed by the detectors at the point of deposit. Two γ-ray detectors [one Ge(Li) and one HpGe] in close 180° geometry were used to collect γ singles, time-sequential γ spectra, and γ-γ coincidence data. A thin plastic scintillator near the tape detected β radiation, and signals from this detector were used as a beam monitor and to provide β gating for the γ singles and time-sequential γ spectra. The β-gate efficiency was about 25%. Spectra that were β gated were free of background γ-rays except for Pb x-rays.

The move cycle for the tape was varied depending on the objective of the experiment. For the half-life measurement the beam was deposited for 1 s followed by a 1-s period during which the beam was deflected and the source was allowed to decay. The tape was then moved a short distance (requiring ~ 0.3 s), and the cycle was repeated. The time-sequential γ spectra were taken only during the 1-s decay portion of the cycle, with the 1-s interval divided into 16 equal time bins. The half-life measurement was made during the first 27 h of experiment 1. For the remainder of experiment 1 and all of experiment 2 the beam was collected during the entire 2-s cycle in order to improve the data-collection rate. The long time-sequential γ experiments used to distinguish γ-rays from the different $A=101$ isobars were taken during beam deposition, and comparison of early and late time bins was generally sufficient for isobar identification. The 2-s growth cycle was used for approximately 140 h in experiment 1 and 80 h in experiment 2.

The various γ-ray singles spectra covered energies up to 4 MeV. The energy calibration was determined by simultaneous measurement of the $A=101$ activity and standard calibration sources. The relative efficiencies of the γ detectors were determined as a function of energy by placing a calibrated standard source on the tape at the point of deposit and counting with the detectors in the experimental geometry. During experiment 1, when the likelihood of primary ^{101}Y contamination in the beam was negligible, a source was collected for 1.5 h with the tape stationary, and a spectrum was then accumulated with all $A=101$ isobars in saturation. This spectrum was used to estimate the ground-state β feeding as discussed in Sec. III.

γ-γ coincidences were accumulated in event mode. The timing signals were produced by a standard fast-coincidence system (employing fast amplifiers and constant-fraction discriminators) and were processed by a time-to-amplitude converter. A time window of ~ 100 ns was used in sorting the data. Altogether 3×10^6 coincidence events were collected during experiment 1 and 11×10^6 events during experiment 2.

C. Half-life of ^{101}Sr

The half-life of ^{101}Sr was determined by following the decay of the strong γ-ray at 128 keV in the time-sequential γ data taken at the beginning of experiment 1. The decay curve for this γ-ray is shown in Fig. 1. A weighted fit to these data yields a half-life of 121 ± 6 ms. This value has been reported in an earlier paper.[12]

D. Determination of γ-ray energy, intensity, and coincidence relationships

A β-gated singles spectrum accumulated during experiment 2 is shown in Fig. 2, while spectra from coincidence gates on the 79-, 128-, and 510-keV γ-rays are shown in Fig. 3. γ energies, relative intensities, placements, and coincidence relationships are contained in Table I. The uncertainties given for the energies are derived from statistical uncertainties in determining peak centroids and system nonlinearities, while uncertainties in the relative intensities derive from uncertainties in determining peak areas and detector efficiencies. No measurable distortion in relative intensities was observed from the β-gate condition. As noted in the table, several of the energy and intensity values were obtained from coincidence data, either because the transition was too weak to appear in singles, was doubly placed in the level scheme, or contained a component from an isobar further down the chain. Transitions below 200 keV were corrected for internal conversion before β feedings were computed, using the proposed level scheme to obtain the most likely multipolarities.

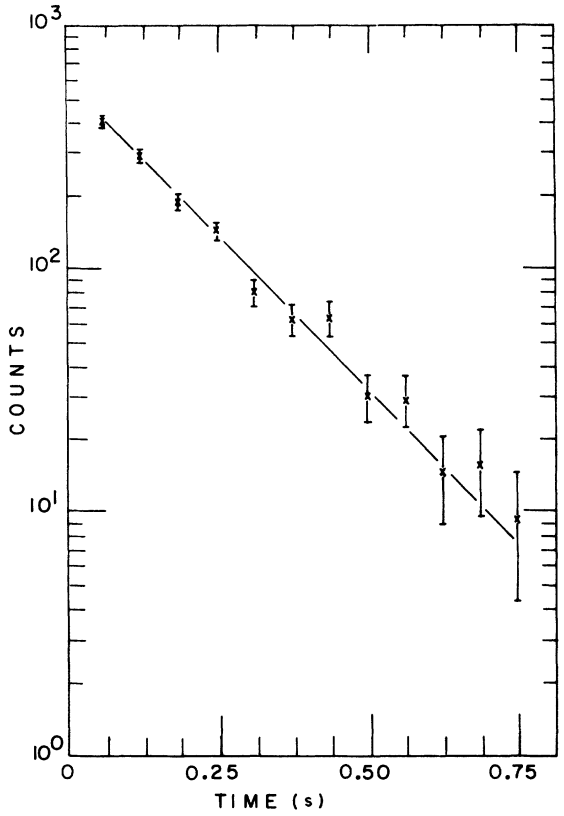

FIG. 1. Decay curve for the 128-keV γ-ray following the decay of ^{101}Sr. The line represents a fit with a half-life of 121±6 ms.

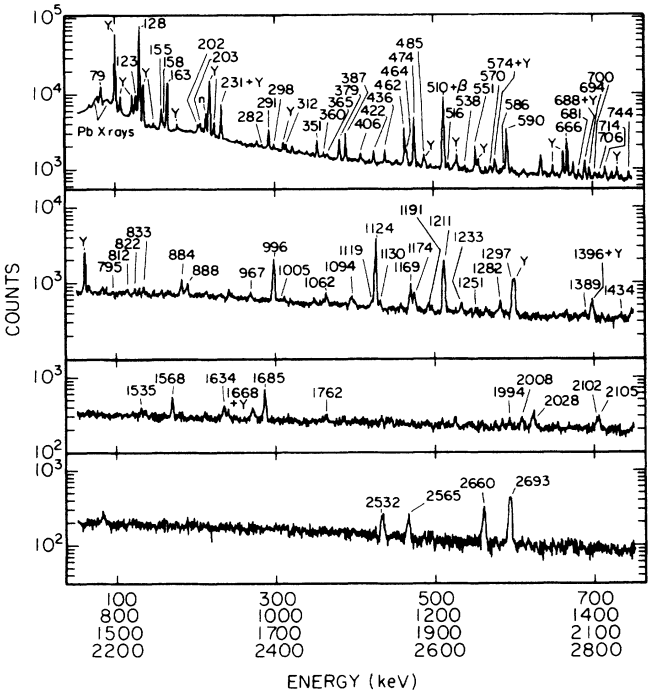

FIG. 2. β-gated γ-ray singles spectrum. ^{101}Sr γ-rays are labeled by their energies in keV. Known γ-rays from the decay of ^{101}Y are labeled by Y and a γ-ray from delayed-neutron emission by n.

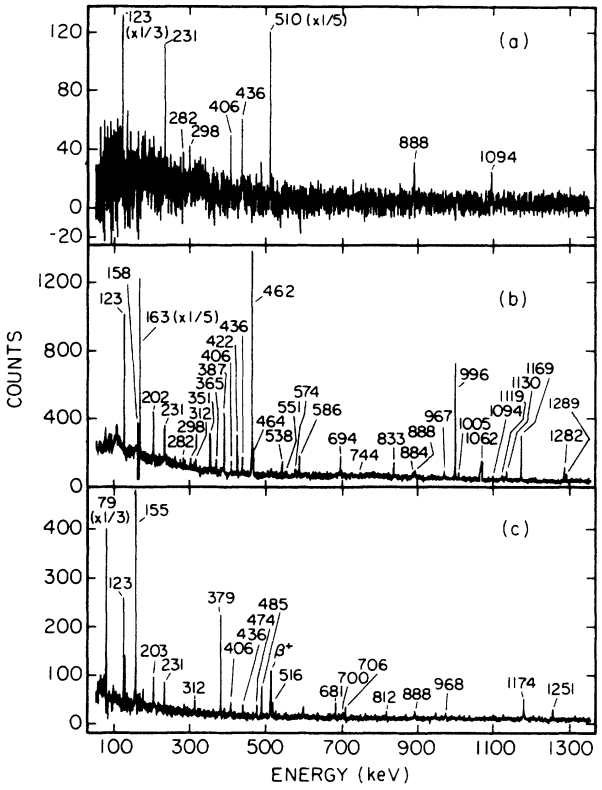

FIG. 3. Coincidence γ-ray spectra from the decay of ^{101}Sr for gates on (a) 79-, (b) 128-, and (c) 510-keV γ-rays. ^{101}Sr γ-rays are labeled by their energies in keV.

III. INTERPRETATION OF RESULTS

A. The ^{101}Sr decay scheme

The level scheme for ^{101}Y from the decay of ^{101}Sr is shown in Fig. 4. It is based on γ-ray singles and coincidence measurements, with placements for individual γ-rays given in Table I. Level energies, β feedings determined from intensity balances, and logft values are given in Table II. In the computation of logft values a ground-state decay energy of 10.0±0.5 MeV was used. This is a calculated value from the mass tables of Möller and Nix.[13] Comparison of measured Q_β values for nearby nuclides with calculated values from the same mass table produced scattered differences consistent with the 0.5-MeV uncertainty assigned above to Q_β.

An estimate of the ground-state β feeding in ^{101}Y has been made from the saturation spectrum as described in Sec. II B. In this spectrum the intensity of the 128-keV γray has been compared with that of the 192-keV γ-ray following the decay of ^{101}Mo. This latter γ-ray has an absolute intensity of (19.6±0.4)% as determined from the ^{101}Mo decay scheme.[14] The comparison results in a value of (35±17)% for the ground-state β branch of ^{101}Sr. The large error is due to the weakness of the two γ-rays in this spectrum and the fact that the 128-keV γ-ray is nearly degenerate with an unknown γ-ray further down the mass chain.

TABLE I. γ transitions observed in ^{101}Sr decay.

E_γ (keV)	I_γ	Placement (keV)	Coincident γ-rays (keV)
79.70±0.05	82±4	590-510	123,231,(282),(298), 406,436,510,888,1094 2102,2105
123.97±0.07	66±5	714-590	79,128,158,298,312,(387), 462,510,590,(1169)
128.34±0.05	1000±50	128-0	123,158,163,202,231,282, 298,312,351,365,387,406, 422,436,462,464,538,551, 574,586,694,744,833,884, 888,967,996,1005,1062, 1094,1119,1130,1169,1282, 1289,1389,1434,1568,1634, 2102,2105,2369,2532,2551, 2565
155.99±0.06	38±4[a]	666-510	510,666,(812)
	5.8±1.9[a]	822-666	
158.43±0.09	18.2±1.8	872-714	79,123,128,163,422,462, 485,510,586,590,714
163.35±0.05	191±10	291-128	128,158,202,298,312,422, 551,833,967,1005,(1094), 1119,1434,1580,2369,2387, 2401
202.63±0.11	18.2±2.1	494-291	128,163,291
203.92±0.20[b]	5.6±1.0[c]	714-510	510
231.89±0.06	9.5±1.5[d]	822-590	79,128,462,510,590
282.73±0.19	5.0±1.0	872-590	79,128,590
291.72±0.07	33±2	291-0	202,422,833,(967)
298.52±0.12	9.1±2.1[e]	1012-714	123,128,(714)
312.87±0.10	15.8±1.5	1027-714	79,123,128,(422),462,510, 586,590,714
351.68±0.08	39±3	1762-1410	128,1282
360.57±0.19	7.5±1.6	1027-666	666
365.97±0.24	5.7±1.3	494-128	128
379.89±0.08	56±3	890-510	510,795
387.77±0.08	73±4	1685-1297	128,1169,1297
406.37±0.12	18.0±2.1	996-590	79,128,462,510,590,(688)
422.84±0.09	31.8±2.4	714-291	128,158,163,291,312
436.98±0.09	32.2±2.3	1027-590	79,128,462,510,590
451.58±0.07	10.4±1.5	1685-1233	1233
462.14±0.08	145±8	590-128	123,128,231,282,406,436, 1094,(2105)
464.77±0.10	39±3	1762-1297	128,1169,1297
474.07±0.08	209±11	1685-1211	510,700,1211
485.85±0.10	28.7±2.4	996-510	510
510.73±0.08	470±30	510-0	79,123,155,203,231, 312,379,406,436,474,485, 516,681,700,706,(812), 888,968,1174,1251
516.36±0.20	10.3±2.1	1027-510	510
538.39±0.10[f]	10.1±1.4[f]	666-128	128
551.01±0.08	71±4	1762-1211	1211
574.1±0.3[g]	9±3[g]	1872-1297	128,1169,1297
586.13±0.15	14.6±2.1	714-128	128,(298),312
590.40±0.08	180±10	590-0	123,158,231,282,312,406, 436,888,1094,1668,2102, 2105
666.60±0.08	144±8	666-0	155,360,812,1205,1994, 2008,2028
681.03±0.19	13.1±2.2	1191-510	510
688.50±0.10	16±5[h]	1685-996	128,406,(462),485,(510)

TABLE I. (*Continued*).

E_γ (keV)	I_γ	Placement (keV)	Coincident γ-rays (keV)
694.33±0.12	24.4±2.5	822-128	128
700.51±0.24	12.9±2.3	1211-510	474,510
706.55±0.18	13.8±2.2	1217-510	510
714.25±0.11	31±3	714-0	158,298,312
744.09±0.17	4.0±1.6[f]	872-128	128
795.1±0.4	8.6±2.4	1685-890	379,510
812.59±0.20	17±3	1479-666	128,155,510,666
822.39±0.17	20±3	822-0	
833.24±0.18	23±3	1124-291	128,163,291
884.8±0.5[f]	5.4±1.6[c]	1012-128	
888.58±0.14	37±3	1479-590	79,128,462,510,590
967.1±0.3	13±4[c,k]	1259-291	128,163,291,510
968.0±0.3	7.0±2.3[c,k]	1479-510	
996.53±0.10	209±11	1124-128	128,1568
1005.4±0.4	9±3	1297-291	128,163,(291)
1010.55±0.18	13.4±2.4	2696-1685	128,474,(1685)
1062.9±0.3	28±8	1191-128	128,570
1094.97±0.20	29±4	1685-590	79,128,462,510,590
1119.39±0.21	25±4	1410-291	128,163,291,351
1124.82±0.11	605±30	1124-0	1535,1568
1130.49±0.21	23±4	1259-128	128
1169.57±0.16	97±11	1297-128	128,387,464,574
1174.44±0.13	64±5	1685-510	510
1191.37±0.07	23.4±1.5	1191-0	No gate
1205.1±0.6[i]	8.4±1.9[i]	1872-666	
1211.28±0.11	339±18	1211-0	474,551,(1463)
1233.45±0.14	32.2±4.4	1233-0	451
1251.31±0.12[c]	19±3[c]	1762-510	510
1282.69±0.18	43±5	1410-128	128,351
1289.92±0.22	12.0±2.3	1418-128	128
1297.61±0.13[l]	86±16[l]	1297-0	387,464,574,1396
1389.48±0.22[f]	14±3[f]	1517-128	128
1396.0±0.5	29±10	2693-1297	128,1169,1297
1411.1±0.3	7.6±1.6	1410-0	No gate
1418.1±0.4	4.1±0.9	1418-0	No gate
1434.66±0.12[b]	21±4[f]	2693-1259	128,163
1463.81±0.20[b]	8.8±1.9[j]	2675-1211	1211
1518.12±0.23	8.7±1.4	1517-0	No gate
1535.5±0.4	15±4	2660-1124	1124
1568.39±0.17	78±6	2693-1124	128,996,1124
1580.5±0.3	5.2±1.2	1872-291	No gate
1634.00±0.19	50±4	1762-128	128
1668.8±0.3	25±4	2259-590	79,128,464,590
1685.32±0.16	133±9	1685-0	
1762.1±0.4	13±3	1762-0	
1994.4±1.0[b]	15±4[i]	2660-666	666
2008.4±0.3	11.6±1.7	2675-666	155,666
2028.1±0.3[b]	14±3[i]	2693-666	666
2102.8±0.9	20±9	2693-590	79,128,462,510,590
2105.6±0.5	38±9	2696-590	79,128,462,510,590
2369.1±0.9	11±5	2660-291	128,163,291
2387.7±1.2[k]	3.8±0.8[k]	2680-291	No gate
2401.8±0.4[b]	6.0±1.0[k]	2693-291	128,163,291
2532.7±0.3	94±8	2660-128	128
2551.9±0.5	8.5±2.0	2680-128	128
2565.4±0.3	91±8	2693-128	128
2660.9±0.3	154±11	2660-0	

TABLE I. (*Continued*).

E_γ (keV)	I_γ	Placement (keV)	Coincident γ-rays (keV)
2675.4±0.6	6.1±1.7	2675-0	No gate
2693.8±0.3	237±13	2693-0	

[a]Derived from singles and the 155- and 666-keV gates.
[b]Derived from a global coincidence spectrum.
[c]Derived from the 510-keV gate.
[d]Derived from the 123- and 590-keV gates.
[e]Derived from the 714-keV gate.
[f]Derived from the 128-keV gate.
[g]Derived from the 1297-keV gate.
[h]Obtained by subtraction of ^{101}Y fraction obtained from the 98-keV gate.
[i]Derived from the 666-keV gate.
[j]Derived from the 1211-keV gate.
[k]Derived from the 163-keV gate.
[l]Derived from the 387-keV gate.

In calculating logft values there is also a systematic error in the total $(\beta+\gamma)$ feeding of the ground state due to an undetermined contribution from possible γ feeding directly to the ground state from unobserved high-energy levels. However, a large uncertainty in the ground-state branching has little effect on logft arguments for allowed β decay, since a ground-state branching as low as 2% would still yield a logft of 5.9 and thus an allowed assignment for this transition. For the excited states, changing the ground-state branching from 35% to 0% changes their logft values by less than 0.2. However, the effect of these unobserved γ-rays populating excited states is of potentially greater significance for an excited state than for the ground state. If an excited state has weak β feeding, then the omission of unobserved incoming γ-rays leads to a deduced β feeding that is too large. Because of such uncertainties, β branching and logft values are given in Table II only for those levels with sufficient β feeding to lead to a deduced logft value of less than 6.0.

The I^π (spin-parity) values shown in Fig. 4 for levels below $\sim$1.5 MeV are based on β feedings, γ-decay patterns, and the rotational-band assignments discussed in Sec. III B. The I^π values in parentheses for 1258- and 1517-keV levels are tentative. For the five levels with log$ft \leq 5.3$, definite I^π values are assigned by assuming allowed β decay and only $M1$, $E1$, or $E2$ γ-rays. This assumption allows the 1762-keV level to be either $3/2^+$ or $5/2^+$, but a tentative $5/2^+$ choice is preferred as discussed in Sec. III C.

B. Arguments for Nilsson assignments

1. *The ground states of ^{101}Sr and ^{101}Y*

In the discussion of rotational-band assignments and other spin and parity assignments made in this section, it is assumed that the ground states of ^{101}Sr and ^{101}Y have I^π values of $3/2^+$ and $5/2^+$, respectively. Although there are no direct measurements to support these assignments, there is strong indirect evidence for them from the present data. A compelling case can be made for the $5/2^+$ assignment to the ^{101}Y ground state (see detailed discussion below) based on fits to the data and on comparison with the well-established[8,9] $\frac{5}{2}$[422] ground-state band in ^{99}Y. It then follows from the low logft for the β decay of ^{101}Sr to this $5/2^+$ ground state of ^{101}Y and from the β-decay pattern to the first two excited states in ^{101}Y (see Table II) that I^π for the ground state of ^{101}Sr is $3/2^+$. Support for this assignment also comes from the study of the $N=61$ and $N=63$ nuclei ^{99}Sr, ^{103}Mo, and ^{105}Mo, where the evidence indicates a $\frac{3}{2}$[411] Nilsson assignment for the last neutron in the ground states of these nuclei.[12,15,16] In fact, an assignment of any other Nilsson orbital lying near the Fermi surface would result in β feedings that would be inconsistent with the β feedings observed in this work. A $3/2^+$ assignment for the ground state of ^{101}Sr thus seems on rather firm ground, with a likely Nilsson assignment of $\frac{3}{2}$[411].

2. *Rotational bands in ^{101}Y*

A Nilsson diagram appropriate for this region is shown in Fig. 5(a). The values $\kappa=0.068$ and $\mu=0.50$ used to generate this diagram are those which produce the excellent agreement discussed in Sec. IV between experimental and calculated bands. Figure 5(b) contains a plot of the single-quasiparticle energies of the Nilsson orbitals for the 39th proton as a function of deformation. As can be seen from this figure, the states nearest the Fermi level for the range of deformations expected in this region $(0.3<\epsilon<0.4)$ are $\frac{5}{2}$[422], $\frac{3}{2}$[301], $\frac{5}{2}$[303], $\frac{3}{2}$[431], $\frac{1}{2}$[431], and $\frac{1}{2}$[301]. In the detailed discussion below, bands associated with $\frac{5}{2}$[422], $\frac{3}{2}$[301], $\frac{5}{2}$[303], and a surprisingly low-lying $\frac{1}{2}$[301] state are proposed for ^{101}Y. Each level below 1.1 MeV is a member of either the $\frac{5}{2}$[422] band or one of the negative-parity bands, as is shown in Fig. 6(a). Major features of these bands are given in Table III. Levels of $\frac{1}{2}$[431] and $\frac{3}{2}$[431] bands

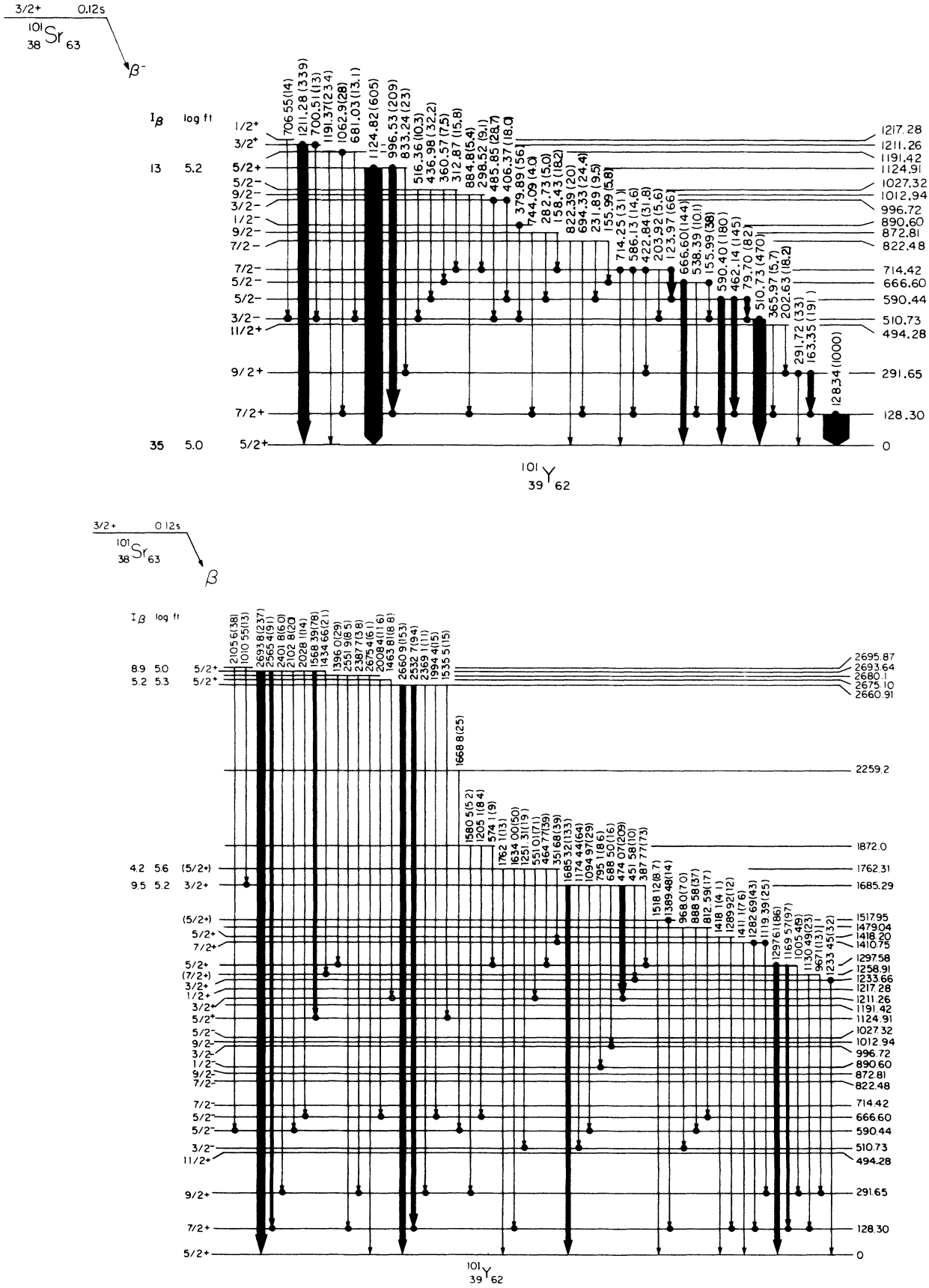

FIG. 4. Decay scheme for ^{101}Sr. β branchings and logft values are shown only for levels with log$ft < 6$. Spin-parity assignments, based on β feedings, γ-decay patterns, and model-dependent rotational-band assignments, are discussed individually in the text.

(and other levels not assigned to bands) lie above 1.1 MeV.

The identified bands were established empirically in several ways. The level energy spacings, β feedings, γ-decay patterns, the assumption of $3/2^+$ for the ground state of ^{101}Sr, and the assignment of the first four levels of ^{101}Y to a $K^\pi = 5/2^+$ rotational band were used to deduce the I^π values for the levels. K values for the bands were deduced by fitting the energy levels of the bands to an axially symmetric rotor whose energy eigenvalues can be approximately expressed in terms of the quantity $J^2=[I(I+1)-K(K+1)]$ by

$$E_{K,I}=E_{K,K}+a\{J^2+bJ^4+a_{2K}[(-)^{I+K}(I+K)!/(I-K)!-(-)^{2K}(2K)!]\}\ ,$$

where $E_{K,K}$ is the bandhead energy, a is the inertial parameter $\hbar^2/2\mathcal{I}$, b is a measure of the rotation-vibration and rotation-particle couplings, and a_{2K} is the "signature term" due to Coriolis coupling. For a nearly rigid rotor b and, for $K\neq\frac{1}{2}$, a_{2K} should both be small compared to unity. For $K=\frac{1}{2}$, a_1 is the usual decoupling parameter whose value may unambiguously characterize the Nilsson orbital, as discussed below for the $\frac{1}{2}$[301] and $\frac{1}{2}$[431] bands. The value of K can often be determined by the level energies of a band.[6]

The intraband γ-decay pattern of a band also provides information that can be used to identify the Nilsson orbital of the band. This can be done by comparing calculated and experimental values of the quantity

$$X=|(g_K-g_R)/Q_0|$$

for different Nilsson orbitals. (g_K and g_R are intrinsic and collective g factors, respectively, and Q_0 is the intrinsic quadrupole moment.) X^2 is proportional to the ratio of $M1$ and $E2$ reduced transition rates,[7] and X is well-determined experimentally by intraband stopover-to-crossover (i.e., $\Delta I=1$ to $\Delta I=2$) γ-ray intensity ratios.

The ground-state $\frac{5}{2}$[422] band. The first four levels in ^{101}Y are very well fit by the assumption that they are members of a $K=\frac{5}{2}$ band. If b and a_{2K} are set to zero, the rms error in the fit to the energy levels is less than 1 keV for $a=18.3$ keV. Only two $K=\frac{5}{2}$ Nilsson states lie near the Fermi surface, $\frac{5}{2}$[422] and $\frac{5}{2}$[303]. The average experimentally deduced value of X is 0.209 ± 0.017 and this is too large by a factor of ~ 10 for the $\frac{5}{2}$[303] choice, for which $X\simeq 0.02$. (Thus, compared to the collective $E2$ crossover γ-rays, the observed stopover γ-rays would be ~ 100 stronger if the band were $\frac{5}{2}$[303].) In Sec. IV the calculated X value, with or without Coriolis mixing, is shown to agree well with experiment for the $\frac{5}{2}$[422] assignment.

The $\frac{3}{2}$[301] and $\frac{5}{2}$[303] bands. From the Nilsson diagram in Fig. 5(a), nearly degenerate low-lying $\frac{5}{2}$[303] and $\frac{3}{2}$[301] bands are expected for ^{101}Y. Such bands have been reported for ^{99}Y and ^{103}Nb.[8,17] We propose that the remaining levels below 1.1 MeV (except for the levels at 890, 996, and 1027 keV) belong to these two bands. (Identification of the latter three levels as members of a $\frac{1}{2}$[301] band is discussed below.) The empirical evidence discussed in the next paragraph is consistent with these assignments. This interpretation is strongly supported by the detailed particle-rotor model calculations given in Sec. IV.

None of the levels in the proposed $\frac{3}{2}$[301] and $\frac{5}{2}$[303] bands receives significant β feeding from the $3/2^+$ ^{101}Sr ground state, consistent with the negative-parity assignments made here. The level at 510 keV de-excites only to the ground state, which indicates $I\leq\frac{3}{2}$ with either parity. (Note that in preliminary work[12] on ^{101}Y, based on weaker activity levels, the 510-keV level was missed because

TABLE II. Level information for ^{101}Sr decay.

Level energy (keV)	Branching[a] (%)	logft[b]
0	35±17	5.0
128.30±0.04		
291.65±0.05		
494.28±0.13		
510.73±0.05		
590.44±0.05		
666.60±0.05		
714.42±0.06		
822.48±0.06		
872.81±0.10		
890.60±0.11		
996.72±0.09		
1012.94±0.15		
1027.32±0.08		
1124.91±0.08	13±4	5.2
1191.42±0.08		
1211.26±0.07		
1217.28±0.22		
1233.66±0.09		
1258.91±0.15		
1297.58±0.08		
1410.75±0.10		
1418.20±0.23		
1479.04±0.14		
1517.95±0.20		
1685.29±0.07	9.5±2.5	5.2
1762.31±0.07	4.1±1.1	5.6
1871.90±0.23		
2259.20±0.3		
2660.91±0.21	5.2±1.4	5.3
2675.10±0.20		
2680.10±0.6		
2693.64±0.12	8.9±2.4	5.0
2695.87±0.21		

[a] β feedings with log$ft>6.0$ are considered unreliable because of possible unobserved γ feeding from above of comparable magnitude to the β branching.

[b] The logft uncertainties are due to the uncertainty in the ground-state branching (see text). Except for the ground state the logft uncertainties are ~ 0.3. For the ground state an asymmetric uncertainty of $+0.5$ and -0.2 is assigned.

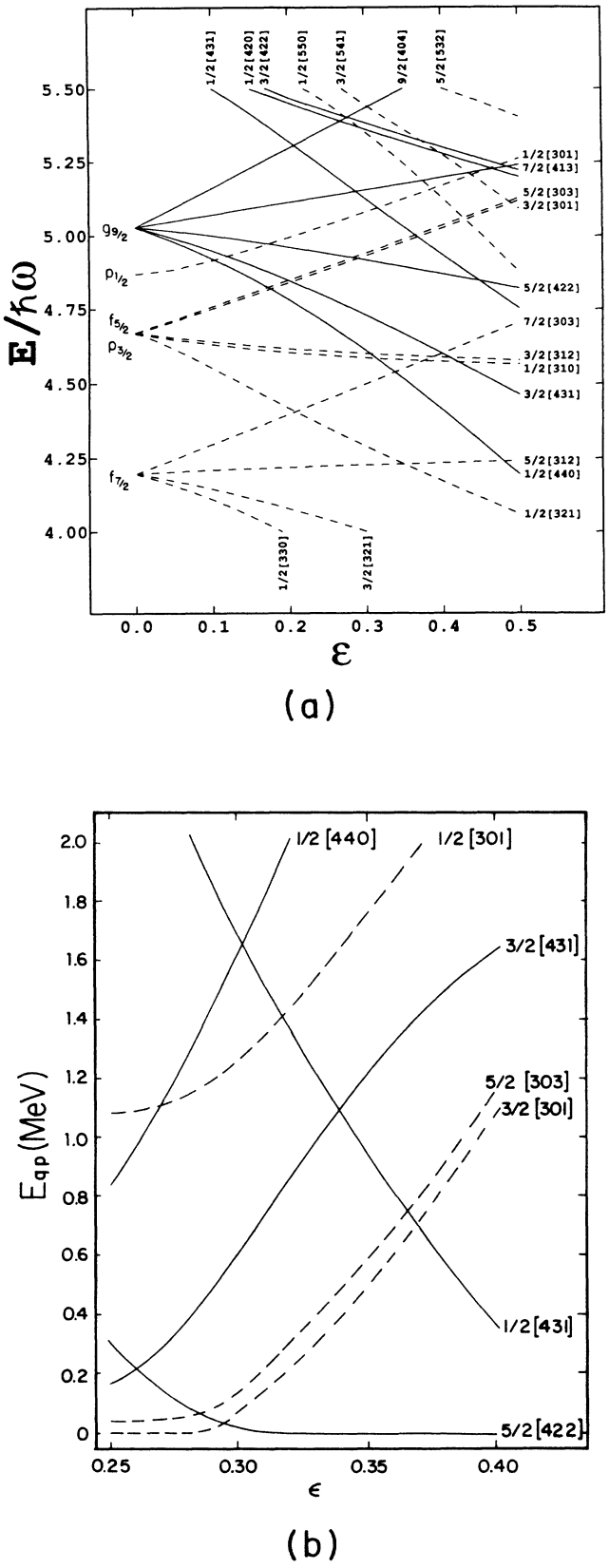

FIG. 5. (a) Nilsson diagram with $\kappa=0.068$ and $\mu=0.50$; (b) quasiparticle excitation energies obtained with $\Delta=0.65$ MeV using normal BCS.

the 510.7-keV γ-ray was masked by more intense 511.0-keV annihilation radiation. This led to the misassignment of the $\frac{5}{2}$ level at 590 keV as a $K=\frac{5}{2}$ bandhead.) For the next two levels at 590 and 666 keV, only an assignment of $I=\frac{5}{2}$ is consistent with the γ-de-excitation patterns observed. Assignments of $I=\frac{7}{2}$ for the levels at 714 and 822 keV and $I=\frac{9}{2}$ for the levels at 872 and 1012 keV are consistent with the experimental data. Note that all interband γ-rays appear to be $M1$ or $E1$ (since $|\Delta I| \leq 1$) and $E2$ γ-rays occur only as intraband γ-rays in the $K=\frac{3}{2}$ band. As is discussed in Sec. IV, the observed intraband $M1$ γ-rays in the $K=\frac{3}{2}$ band rule out the possibility that this band could be $\frac{3}{2}$[431].

Each of the negative-parity levels listed above is assigned to one of the two bands $\frac{3}{2}$[301] and $\frac{5}{2}$[303]. Placement of the $3/2^-$ $\frac{3}{2}$[301] bandhead at 510 keV is unambiguous. A naive assumption of no Coriolis mixing of these bands would make the 510-, 590-, 714-, 872-keV levels the obvious choice for the $\frac{3}{2}$[301] band, with the levels 666, 822, 1012 keV forming the $\frac{5}{2}$[303] band. This is the choice shown in Fig. 6. Using the rotor energy equation with both b and a_{2K} set to 0 gives inertial parameters $a=16.0$ keV for the $\frac{3}{2}$[301] band and $a=22.3$ keV for the $\frac{5}{2}$[303] band. (If each unmixed band had an intermediate a value of ~ 20 keV, then Coriolis mixing of the two bands could give the above a values as well as explain small deviations from the simple energy formula.) For the 510-590-714-872 choice for the $\frac{3}{2}$[301] band, the average experimental X is 0.38 ± 0.07, in excellent agreement with the X value expected (see Ref. 7 or Sec. IV) for an unmixed $\frac{3}{2}$[301] band. (The other choice for a $K=\frac{3}{2}$ band (i.e., 510-666-822-1012 keV) does not yield an X value remotely similar to that expected for a $\frac{3}{2}$[301] band.) The absence of an $E2$ crossover transition in the proposed $\frac{5}{2}$[303] band precludes extraction of an experimental X value for this band. The Coriolis mixing calculations in Sec. IV adds further support to the assignments deduced here.

The $\frac{1}{2}$[301] band. As already noted, the appearance of a $\frac{1}{2}^-$ bandhead at such a low energy (890 keV) is surprising since there does not appear to be a Nilsson candidate for a $1/2^-$ state very near the Fermi level. The lowest-lying $1/2^-$ state is $\frac{1}{2}$[301] which is predicted (see Fig. 5) at an excitation energy of about 1.5 MeV. However, the observed γ-decay pattern and deduced decoupling parameter provide a clear identification of the levels at 890, 996, and 1027 keV as the first three members of a $\frac{1}{2}$[301] band. With b set to 0, a fit to the three levels gives $a=20.8$ keV and $a_1=+0.70$. As expected, this value of a is close to the estimated "unmixed" value of ~ 20 keV for the two lower-lying negative-parity bands. As Fig. 7 shows, the deduced value of a_1 is in excellent agreement with the $\frac{1}{2}$[301] assignment. The only other $K=\frac{1}{2}$ orbitals with a_1 values close to $+0.70$ are $\frac{1}{2}$[420] and $\frac{1}{2}$[321], but (as can be seen in Fig. 5) these orbitals both lie ~ 4 MeV from the Fermi surface, so they are not viable candidates for the observed band.

The γ-decay pattern for members of a $\frac{1}{2}$[301] band

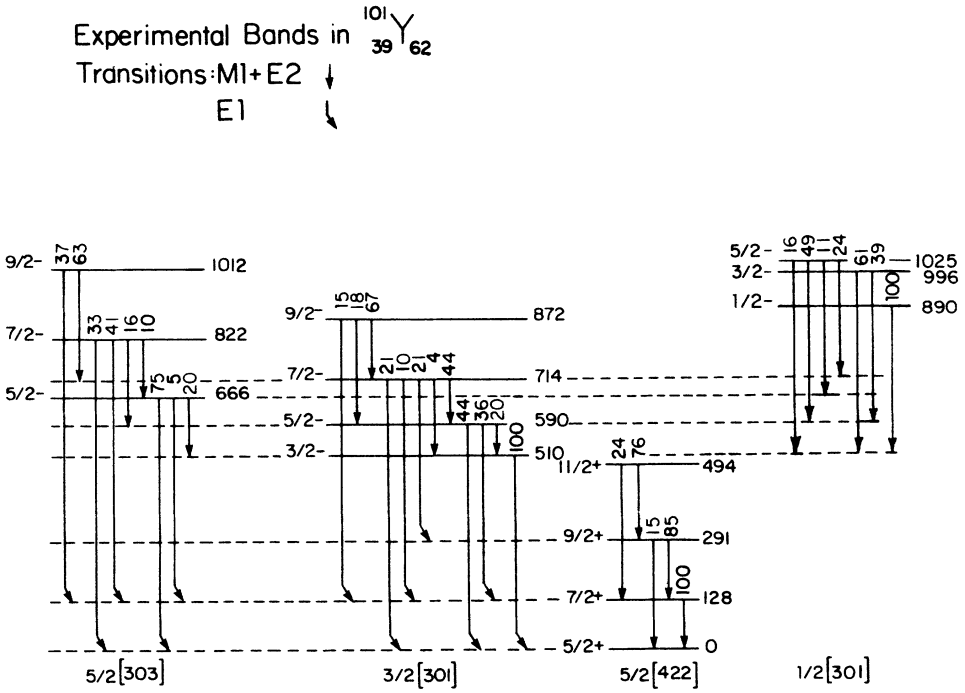

FIG. 6. Experimental rotational bands and relative γ-ray intensities for levels in ^{101}Y. The four bands contain all levels below 1.1 MeV.

should be dominated by $M1$ γ-rays to the $\frac{3}{2}$[301] band, and the intensity ratios of the $M1$ γ-rays from a given level should be determined solely by Alaga rules for dipoles. The observed γ-decay pattern between the $\frac{1}{2}$[301] and $\frac{3}{2}$[303] bands are in excellent agreement with the Alaga rules. There should be no γ-rays from the $\frac{1}{2}$[301] to the $\frac{5}{2}$[303] band (due to K forbiddeness) in the absence of Coriolis mixing between the $\frac{5}{2}$[303] and $\frac{3}{2}$[301] bands. The observed (weaker) γ-rays from the $\frac{1}{2}$[301] band to the $\frac{5}{2}$[303] band give an additional (and independent) indication of Coriolis mixing of the close-lying $\frac{3}{2}$[301] and $\frac{5}{2}$[303] bands. Even though it occurs lower in energy than expected, the evidence in support of the proposed $\frac{1}{2}$[301] band is strong.

Excited, positive-parity bands. Reference to Fig. 5 suggests that positive-parity bands with K^π values of $1/2^+$ and $3/2^+$ might be expected at excitation energies of 1 to 1.5 MeV. Several experimental levels in this energy range (1211, 1217, 1233, 1259, 1297, 1410, 1418, and 1518 keV) have γ-decay patterns that would be consistent with tran-

TABLE III. Major features of bands in ^{99}Y (Ref. 7) and ^{101}Y.

Nilsson orbital		Bandhead (keV)	$a=\hbar^2/2\mathcal{I}$ (keV)	a_1[a]	Pattern of γ-ray deexcitations
$\frac{5}{2}$[422]	^{99}Y:	0	17.9		$M1 \gg E2$
	^{101}Y:	0	18.3		$M1 \gg E2$
$\frac{3}{2}$[301]	^{99}Y:	536	23.6		$E1 \sim M1 > E2$
	^{101}Y:	510	16.0		$E1 \sim M1 > E2$
$\frac{5}{2}$[303]	^{99}Y:	487	19.6		$E1 \gg E2 > M1$
	^{101}Y:	666	22.3		$E1 \sim M1 > E2$
$\frac{1}{2}$[301][b]	^{99}Y:				
	^{101}Y:	890	20.8	0.70	$M1 \gg E1, E2$
$\frac{1}{2}$[431]	^{99}Y:	1011	17.8	−1.05	$M1 \gg E1, E2$
	^{101}Y:	1217[c]	20.3 21.2	−1.10 −0.74	$M1 \gg E1, E2$

[a]Decoupling parameter a_1 given only for $K=\frac{1}{2}$ bands.

[b]$\frac{1}{2}$[301] band not identified in ^{99}Y.

[c]Two choices of a and a_1 values for $\frac{1}{2}$[431] band in ^{101}Y.

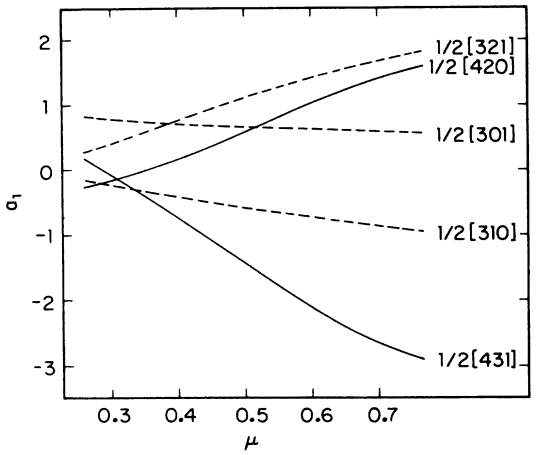

FIG. 7. Decoupling parameter a_1 for selected $K=\frac{1}{2}$ bands calculated with $\kappa=0.068$ and deformation $\epsilon=0.35$. Not shown are bands $\frac{1}{2}$[440] and $\frac{1}{2}$[550] with a_1 values outside the range of the plot.

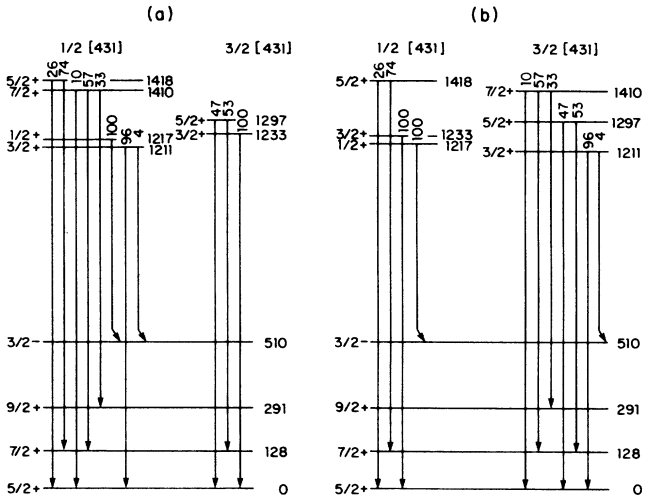

FIG. 8. Two possible assignments of experimental levels in ^{101}Y to the bands $\frac{1}{2}$[431] and $\frac{3}{2}$[431]: (a) with $3/2^+$ member of $\frac{1}{2}$[431] band at 1211 keV, corresponding to $a_1=-1.10$; (b) with $3/2^+$ member of $\frac{1}{2}$[431] band at 1233 keV, corresponding to $a_1=-0.74$.

sitions from members of such bands to levels in the four lower-lying bands. With the exception of a level at 1124 keV, no level in this range has significant β feeding, which is consistent (according to the modified Alaga rules for allowed hindered β transitions[18]) with expectations for β decay of a $\frac{3}{2}$[411] neutron to members of $\frac{3}{2}$[431] and $\frac{1}{2}$[431] bands in ^{101}Y. If levels in this energy range are members of $\frac{3}{2}$[431] and $\frac{1}{2}$[431] bands, then their close proximity in energy could result in significant Coriolis mixing and thus possible distortion of the level energies. More significantly, however, Coriolis mixing would have a large effect on the $M1$ γ-rays from the mixed $\frac{1}{2}$[431] band to the $\frac{5}{2}$[422] ground band since such $M1$ γ-rays would otherwise by K forbidden.

Among the levels listed above only the level at 1217 keV is a candidate for the $\frac{1}{2}$[431] bandhead. It de-excites by a single γ-ray to the $3/2^-$ level at 510 keV, as expected for a level with $I^\pi=1/2^+$. Levels at 1211 and 1233 keV de-excite only to the ground state, as expected for $3/2^+$ levels, and are thus candidates for the $\frac{3}{2}$[431] bandhead. For $I>\frac{3}{2}$, the dipole Alaga rules provide reasonable "expectations" for γ-decay patterns. The levels at 1297, 1418, and 1518 keV have γ-decay patterns expected for $5/2^+$ levels, while the levels at 1259 and 1410 keV have γ-decay patterns expected for $7/2^+$ levels.

There are two viable choices for assigning some of the above levels to the $\frac{1}{2}$[431] and $\frac{3}{2}$[431] bands. The band patterns that result from these two choices are shown in Fig. 8. For either choice, the 1217-keV level is the $\frac{1}{2}$[431] bandhead. Neither choice involves the $7/2^+$ level at 1259 keV and the $5/2^+$ level at 1518 keV, since these energies are, respectively, two low and too high to belong to either of the two bands. In discussing the patterns of Fig. 8, it is useful to recall the expected values of the Nilsson and rotor parameters that were deduced for the four lower-lying bands. All four lower-lying bands indicate a core inertial parameter a_0 of $\simeq$20 keV. The three negative-parity bands are consistent with a Nilsson μ value of $\sim$0.5 and a deformation ϵ of $\sim$0.35. As Fig. 7 shows, the value of a_1 for the $\frac{1}{2}$[431] band is thus expected to be slightly more negative than -1.

Figure 8(a) shows four members of a $\frac{1}{2}$[431] band with level energies that are both internally consistent and agree well with the above "expected" values of a and a_1. Internal consistency is illustrated by using the rotor-energy expression to fit the energies of the $3/2^+$, $5/2^+$, and $7/2^+$ levels relative to the $1/2^+$ bandhead. The results of this fit are $a_0=19.9$ keV and $a_1=-1.07$ with an rms deviation of only 1.7 keV. These values of a_0 and a_1 are in excellent agreement with the above expectations. However, the remaining levels ($3/2^+$ at 1233 keV and $5/2^+$ at 1297 keV) lie too close together to belong to the $\frac{3}{2}$[431] band. Their level spacing of 64 keV indicates an inertial parameter of only 13 keV, which is so low that it implies a moment of inertia larger than the rigid value. It is, of course, possible that the γ-rays (thus the levels) of a $\frac{3}{2}$[431] band have not been identified. Weak β feeding or masking by other $A=101$ γ-rays are possible, particularly for the $3/2^+$ bandhead, since it would de-excite only to the $5/2^+$ ground state and thus may not be observed in γ-γ coincidence spectra.

Figure 8(b) shows three members in each band, with a $\frac{3}{2}$[431] band having an inertial parameter a of $\sim$17 keV. The parameters deduced from the three levels of the $\frac{1}{2}$[431] band in Fig. 8(b) are $a=21.2$ keV and $a_1=-0.74$. These two a values are not unreasonable, but the a_1 value corresponds to a lower value of the Nilsson parameter μ than is indicated by the three lower-lying negative-parity bands. It is possible that the negative- and positive-parity bands can have different

values of μ, but the only experimental indication of this would be the $\frac{1}{2}[431]$ band shown in Fig. 8(b).

At present we have insufficient experimental information to justify a choice of one of the two patterns shown in Fig. 8. Thus the position of the expected $\frac{3}{2}[431]$ band remains unclear. Only the $\frac{1}{2}[431]$ bandhead energy is unambigous. Table III gives both sets of parameters a and a_1, corresponding to the two choices of Fig. 8. As is discussed in detail in Sec. IV, however, if any of the above levels with $I \geq 3/2$ are members of the $\frac{1}{2}[431]$ band, then their γ-decay patterns indicate the $\frac{3}{2}[431]$ band lies near enough in energy so that Coriolis mixing of the two bands can give the observed $\frac{1}{2}[431]$ γ-decay patterns to the $\frac{5}{2}[422]$ ground band. With the inclusion of Coriolis mixing in the particle-rotor calculations of Sec. IV, either of the two Fig. 8 patterns can be obtained. Both are discussed in Sec. IV.

C. Other levels in ^{101}Y

There are several other levels not among those considered above that have properties with interesting structure implications for $A \sim 100$ nuclei. The levels to be discussed in this section are strongly β fed, receiving more than 40% of the total β feeding. In addition, γ-decay patterns from these levels also indicate that they are strongly coupled to the $\frac{5}{2}[422]$ band.

1124-keV level. This level has the strongest β feeding of any of the excited levels and a logft of 5.2. The very low logft classifies this β transition as allowed unhindered under the modified Alaga rules.[18] γ-deexcitation occurs only to the first three members of the ground-state band. This γ-decay pattern, combined with the strong β feeding, limits the spin and parity of the level to $5/2^+$. The strong coupling of this state through β decay from the $\frac{3}{2}[411]$ ground state of ^{101}Sr and through γ decay to the $\frac{5}{2}[422]$ ground band of ^{101}Y would be explained if the 1124-keV level were to have a significant $\frac{5}{2}[422]$ component. For example, the state could be a $\frac{5}{2}[422]$ proton coupled to the 0^+ first β vibration of the deformed core.

Levels at 1685, 1762, and 1872 keV. These three levels are curious because they have the energy signature of a pure $K = \frac{3}{2}$ band with $a = 15.4$ keV. The first two levels are strongly β fed while the level at 1872 keV is not. This pattern of β feeding and the observed γ-decay patterns support $3/2^+$, $5/2^+$, and $7/2^+$ assignments to the levels, respectively. The logft value for the 1685-keV level is characteristic of an unhindered or nearly unhindered[18] allowed β transition. There are no single-quasiparticle $K = \frac{3}{2}$ states near the Fermi level (except for $\frac{3}{2}[431]$) that could be identified with this band. At this energy, a three-quasiparticle $K = \frac{3}{2}$ configuration such as

$$\{\pi\tfrac{5}{2}[422], \nu\tfrac{3}{2}[411], (\nu\tfrac{3}{2}[422])^{-1}\}$$

is a likely choice, since its $\pi\frac{5}{2}[422]$ component could account for the low-logft β transitions from the $\nu\frac{3}{2}[411]$ ground state of ^{101}Sr.

Levels around 2.6 MeV. There is a very closely spaced cluster of five rather isolated levels between 2660 and 2696 keV. No levels are observed above these, and there are only three levels in the 1-MeV energy interval below them. Two of the levels, at 2660 and 2693 MeV, receive substantial β feeding, with logft values that suggest allowed unhindered β transitions. The strong β feeding and the fact that both of these levels are strongly coupled to the ground band (with γ-rays to the first three members of the ground band) requires an I^π value of $5/2^+$. Possible explanations for these states would include three-quasiparticle structures involving the $\frac{5}{2}[422]$ Nilsson state as discussed above or phonon states (β or γ vibrations of the even-even core) coupled to the $\frac{5}{2}[422]$ ground state.

IV. PARTICLE-ROTOR MODEL CALCULATIONS

A. Results for ^{101}Y

The particle-rotor model uses single quasiparticles (with BCS pairing and Coriolis mixing) to calculate the experimentally deduced bands, energy levels, and γ-ray-decay patterns. This calculation gives a self-consistent interpretation of the structure of ^{101}Y. Details of the calculation are given in Ref. 7 and are only briefly reviewed here. The calculation involves a number of parameters, some of which can be determined by consideration of other data. The pairing strength Δ is deduced (from mass measurements on neutron-rich Rb isotopes[19]) to be about half the global value of $12/A^{1/2}$ MeV. Estimates of the Nilsson parameters κ and μ are obtained from single-quasiparticle data for Y nuclei near stability. The deformation ϵ and the inertial parameter a_0 of the core are assumed to be essentially the same as for the more deformed even-even $A \sim 100$ nuclei, such as ^{100}Sr. With the assumed axial symmetry, the quadrupole moment Q_0 is deduced from ϵ. Slight adjustments in the parameters Δ, κ, μ, ϵ, and a_0 provide a better fit to the bandhead energies, but once chosen these parameters are fixed for all bands.

The quasiparticle parameters (Δ, κ, μ, and ϵ) for ^{101}Y are similar to those used in Ref. 7. The specific values of these parameters depend upon the BCS pairing model used. In Ref. 7, the "normal" BCS model (without blocking effects) was used and the quasiparticle parameters were varied to reproduce the bandhead energies. Subsequently, we have investigated the effects of using instead either the BCS version of Kumar *et al.*[20] or BCS with full inclusion of blocking effects, as described by Ogle *et al.*[21] (In these two versions, the parameter G replaces the gap parameter Δ.) The BCS version of Ref. 20 gives a partial correction and that of Ref. 21 a full correction of the well-known compression effect of the normal BCS model on the low-lying quasiparticle energies. Consequently, in order to get the same quasiparticle energies, a different set of these parameters is needed for each BCS version.

The parameter set (Δ, κ, μ, and ϵ) is also affected by the choice of the recoil term in the zero-point rotational energy. To each bandhead this adds the energy $a_0\gamma(K)$, where $\gamma(K) \simeq (\langle K \mid j^2 \mid K \rangle - K^2)$.[21] In the review paper of Ogle *et al.*,[21] the estimate of 0.5 K^2 was used for $\gamma(K)$.

We have also calculated $\gamma(K)$ for each Nilsson orbital and found significant variations from the 0.5 K^2 estimate, especially for unique-parity orbitals. (Such large variations were reported earlier by Popli *et al.*[22]) How $\gamma(K)$ and BCS are treated both affect the deduced quasiparticle parameter set. There are thus many sets of values of Δ, κ, μ, and ϵ that are equivalent as far as bandhead energies are concerned. It is important to emphasize, however, that the ambiguity in these parameters has no effect (other than the decoupling parameter a_1) on energy levels within a band and very little effect on the calculated γ-decay patterns. Therefore, in calculations that reproduce the experimental bandhead energies, the essential properties of the bands can be obtained by the expedient of adjusting quasiparticle energies to get the desired bandhead energies. This procedure is preferred to the alternative procedure (used in Ref. 7) of making a BCS and $\gamma(K)$ choice and then iterating the parameters Δ, κ, μ, and ϵ in order to reproduce bandhead energies.

In fitting energy levels within the bands, a scale parameter k, which multiplies the nondiagonal Coriolis matrix elements, is used. (k is the Coriolis parameter described by Bunker and Reich[6] in their discussion of rotational bands in rare-earth nuclei, where the values of k are of the order of unity but are usually less than unity for unique-parity bands.) The choice of energy parameters Δ, κ, μ, ϵ, and k that best fits the energy levels also fixes the Coriolis mixing between the bands. Only then are γ-ray intensities for all levels in the bands calculated. Two γ-ray parameters, g' (which multiplies the free proton spin factor g_s^{free} to give an effective value $g_s^{\text{eff}}=g'g_s^{\text{free}}$) and the $E1$ scale factor H (which multiplies the $E1$ matrix element) are determined by reproducing the observed γ-decay patterns.

The basic philosophy of the calculations is to minimize the number of variable parameters by imposing constraints on them. One constraint is the requirement that all bands have the same values of the parameters Δ, κ, μ, ϵ, a_0, and Q_0. Other constraints are that all unique-parity bands have the same k and g' values, and similarly for all normal-parity bands. All $\Delta K=0$ $E1$ γ-rays are constrained to have the same factor H, as are all $\Delta K=\pm 1$ $E1$ γ-rays. By minimizing the number of parameters, the calculations are able to describe the observed bands provided that the correct Nilsson assignments are made. (This would not be true if, for example, parameters describing each band were arbitrarily adjusted, for then it might be possible to force nearly any preconceived Nilsson assignments upon the bands.)

Figure 9 gives the results of a ^{101}Y calculation for the lowest four bands. (Although the bands shown in Fig. 9 were calculated using the normal BCS version with $\Delta=0.65$ MeV, nearly identical results can also be obtained using the Kumar *et al.*[20] or blocking[21] BCS versions.) In these calculations the core inertial parameter a_0 is 20.4 keV for all bands. The Coriolis parameter k is 1.15 for negative-parity bands and 0.60 for the positive-parity bands. The γ-ray parameters are $g'=0.70$ for either parity, $H=-0.3$ for $\Delta K=\pm 1$ γ-rays, and $H=2.7$ for $\Delta K=0$ γ-rays. Because of the constraints imposed, and since the number of levels exceeds the available energy parameters and the number of γ-ray relative intensi-

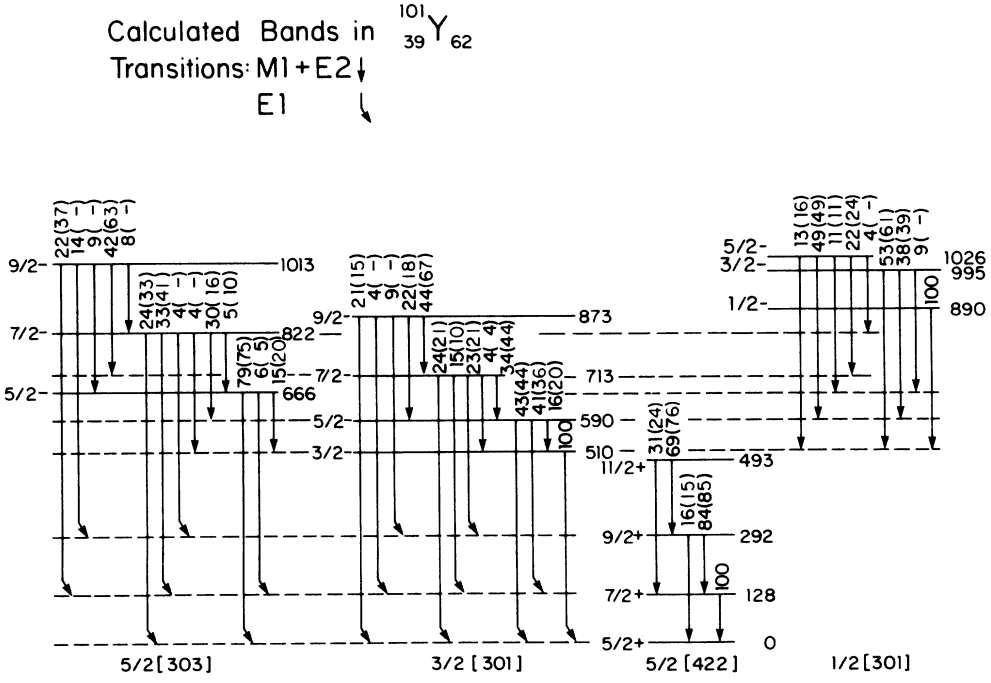

FIG. 9. Calculated levels and relative γ-ray intensities for the four lower bands in ^{101}Y. For ease of comparison with the four corresponding experimental bands shown in Fig. 6, the experimental γ-ray intensities are given in parentheses, with a – (dash) for an unobserved γ-ray.

ties far exceeds the available γ-ray parameters, both types of parameters are overdetermined. Comparison of Fig. 9 with the experimental bands of Fig. 6 shows that the level energies agree within 1 keV. Of greater significance to correct Nilsson assignments, the experimental γ-decay patterns are also well reproduced. We conclude that the calculations establish the Nilsson assignments of these four bands.

Several details of the ^{101}Y calculation are worth noting. The a_0 value of 20.4 keV is strongly influenced by the $\frac{1}{2}$[301] band since this band has little Coriolis mixing. (It is too isolated in energy for the relatively weak Coriolis matrix elements to produce much mixing with other normal-parity bands.) With $a_0=20.4$ keV, an accurate reproduction of the observed spacings in the $\frac{3}{2}$[301] and $\frac{5}{2}$[303] bands requires $k=1.15$ for normal-parity bands. Also, with this a_0, the ground-band energy spacings imply $k=0.60$ for unique-parity bands. The calculated $\frac{1}{2}$[301] γ-decay pattern is parameter free since it is due only to the $M1$ matrix element between $\frac{1}{2}$[301] and $\frac{3}{2}$[301]. The γ-rays from the $\frac{1}{2}$[301] band to the $\frac{5}{2}$[303] band merely confirm the calculated admixtures of $\frac{3}{2}$[301] in the $\frac{5}{2}$[303] band.

Table IV illustrates the effects of Coriolis mixing on intraband γ-rays. Although the effective $(g_K-g_R)/Q_0$ for a mixed band is not constant (Coriolis mixing tends to increase with I), use of a constant effective $(g_K-g_R)/Q_0$ gives an approximate description of a mixed band. The $M1$ strengths in the intraband γ-decays of the $\frac{5}{2}$[422] and $\frac{3}{2}$[301] bands are reduced by Coriolis mixing, but the effect is rather small and the calculated values, either with or without mixing, are consistent with the experimental $(g_K-g_R)/Q_0$ values. For the $\frac{5}{2}$[303] band, however, the $M1$ strengths for intraband γ-rays are increased significantly due to $\frac{3}{2}$[301] admixtures but are still weak in comparison to the interband $M1$ γ-rays. All aspects of the Coriolis-mixed $\frac{3}{2}$[301] and $\frac{5}{2}$[303] bands that are discussed qualitatively in Sec. III are reproduced quantitatively. The three γ-ray parameters (g' and the two H values) are overdetermined by the 20 observed γ-rays from the six levels with $I>\frac{3}{2}$ in the $\frac{3}{2}$[301] and $\frac{5}{2}$[303] bands.

Figure 10 shows the results of two calculations for the $\frac{1}{2}$[431] and $\frac{3}{2}$[431] bands. Although adjustments of a few keV in quasiparticle energies were made to get a $1/2^+$ level at 1217 keV and a $5/2^+$ level at 1297 keV, the main difference is the value of the decoupling parameter a_1 for the $\frac{1}{2}$[431] band. In Fig. 10(a) the $3/2^+$ member of the $\frac{1}{2}$[431] band occurs at 1211 keV, giving an effective (i.e., after Coriolis mixing) a_1 of -1.10, for an unmixed a_1 of -1.04. In Fig. 10(b) the $3/2^+$ member of this band occurs at 1233 keV, giving an effective a_1 of -0.74, for an unmixed a_1 of -0.73. In both cases the two $3/2^+$ levels have significant ($\sim 10\%$) Coriolis mixing and the most mixing ($\sim 20\%$) occurs between the two $7/2^+$ levels. The $5/2^+$ levels, being farther apart in energy, have mixing of only $\sim 1\%$, but this is more than is needed to explain the observed γ-decay pattern from the $5/2^+$ level of the mixed $\frac{1}{2}$[431] band. In fact, the calculations show that an admixture of only 0.4% in this $5/2^+$ level permits the $M1$ γ-rays to the ground band to be more intense than (experimentally unobserved) $E1$ γ-rays to the negative-parity bands. For both calculations, spacings between levels in the $\frac{3}{2}$[431] band are greater than for the corresponding cases in Fig. 8, although the discrepancy is less for case (b). For the $\frac{1}{2}$[431] band, case (a) agrees more closely with the levels in Fig. 8. The calculations do not suggest a clear choice between the two cases. A clear choice may be possible in the future, if more information on deformed odd-Z $A\sim 100$ nuclei indicates the appropriate a_1 value for the $\frac{1}{2}$[431] band.

An unanticipated result of this study of ^{101}Y was the low energy of the $\frac{1}{2}$[301] band. With $\mu\sim 0.5$ (as suggested by the bandhead energy difference of the $\frac{3}{2}$[301] and $\frac{5}{2}$[303] bands or the a_1 value of the $\frac{1}{2}$[301] band) the $\frac{1}{2}$[301] band is calculated to lie closer to 1.5 MeV than

TABLE IV. Calculated and experimental values of intraband parameter $(g_K-g_R)/Q_0$ for the three lowest bands in ^{101}Y.

Nilsson orbital	Spin of upper level	Experimental[a] $X=\lvert(g_K-g_R)/Q_0\rvert$	Calculated[b] $(g_K-g_R)/Q_0$ For unmixed pure-K band	Effective[a] (with mixing)
$\frac{5}{2}$[422]	$\frac{9}{2}$	0.20±0.02	0.254	0.223
	$\frac{11}{2}$	0.23±0.03	0.254	0.224
$\frac{3}{2}$[301]	$\frac{7}{2}$	0.33±0.04	0.361	0.296
	$\frac{9}{2}$	0.34±0.05	0.361	0.271
$\frac{5}{2}$[303]	$\frac{9}{2}$		0.021	0.087
	$\frac{11}{2}$		0.021	0.095

[a]The experimental and effective $(g_K-g_R)/Q_0$ parameters are deduced by fitting a γ-ray crossover-to-stopover branching ratio to the equation for a pure-K band.
[b]$Q_0=4.2$ b and $g'=0.7$ for the calculated $M1$ and $E2$ matrix elements.

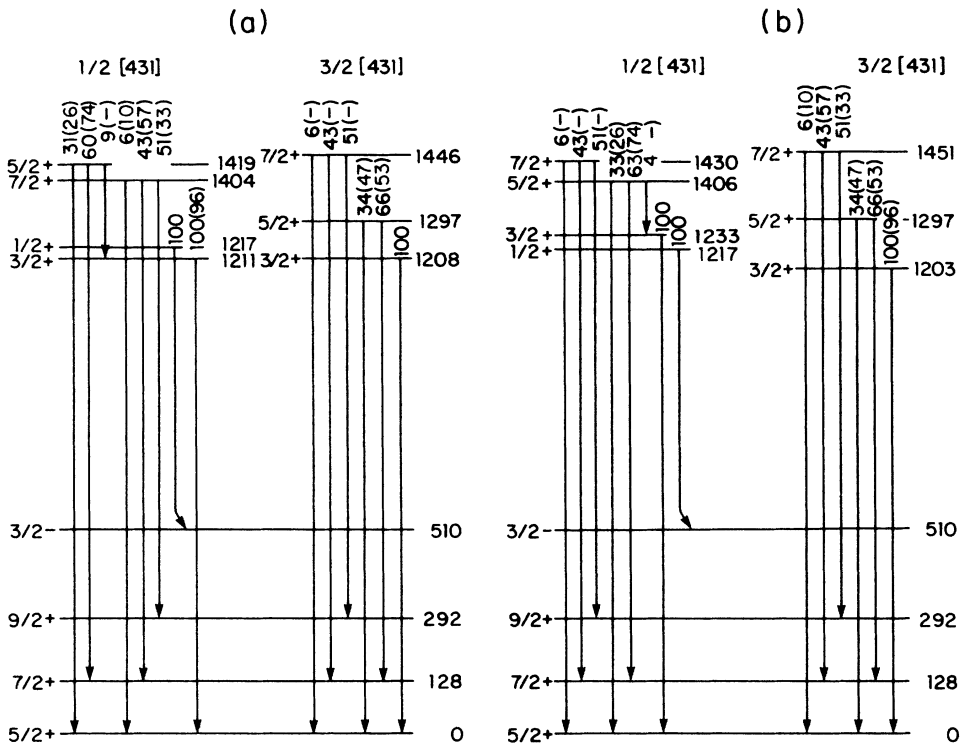

FIG. 10. Calculated analog to Fig. 8, with experimental γ-ray intensities given in parentheses. The γ-rays from $\frac{1}{2}[431]$ levels with $I \geq \frac{3}{2}$ are $M1$ γ-rays connecting $\frac{3}{2}[431]$ admixtures to the ground band.

0.9 MeV, thus its quasiparticle energy was lowered significantly in the current calculation. One alternative would be different quasiparticle parameters (Δ, κ, μ, and ϵ) that could lower this band without adversely affecting the other bandheads. Indeed, μ values as low as 0.4 (Ref. 23) and as high as 0.64 (Ref. 24) have been suggested. Another alternative, mentioned earlier in this section, would be to abandon the usual BCS particle-number constraint and use the Fermi energy as an additional quasiparticle parameter.[22] It is also possible that the problem is not in the parameter set but in the Hamiltonian for the particle-rotor model with BCS pairing used here. However, in spite of the parameter or model ambiguities, the present analysis clearly shows that γ-decay patterns are of crucial importance in determining the proper Nilsson assignments of the observed rotational bands and that Coriolis mixing cannot be neglected in interpreting these γ-decay patterns.

B. Comparison of ^{101}Y and ^{99}Y

A comparison of the level structures and particle-rotor calculations for ^{99}Y and ^{101}Y reveals a remarkable similarity in the structure of the two isotopes. The difference of two neutrons apparently has little influence on their structure, which is dominated by the single-particle characteristics of the odd proton and a deformed core whose character closely resembles that of the even-even nuclei with $A \sim 40$ and $N \geq 60$. Figure 11(a) gives the low-energy structure of ^{99}Y as reported in Ref. 8. Figure 11(b) gives the results of the particle-rotor calculation of Ref. 7. It should be noted that although the fission yield is much greater for ^{99}Sr than for ^{101}Sr, the present results are based on better data than were obtained for the ^{99}Sr decay study because of the superior ion sources available for the present study. Thus there is greater confidence in the present work. The major difference between Ref. 8 and the present work involves the $\frac{1}{2}[431]$ and $\frac{3}{2}[431]$ bands. It is likely that an error was made in Refs. 7 and 8 in the identification of the $\frac{3}{2}[431]$ band in ^{99}Y. This is discussed further below.

The lowest-lying levels in both Y isotopes consist mainly of rotational bands based on the Nilsson states $\frac{5}{2}[422]$, $\frac{3}{2}[301]$, and $\frac{5}{2}[303]$. It is of interest to note that these same three bands also apparently account for the low-lying levels in ^{103}Nb.[17] The four lowest members of the $\frac{5}{2}[422]$ ground band in ^{99}Y and ^{101}Y are nearly identical in their energies and γ-decay patterns, and this also extends to ^{103}Nb (with band members at 0, 126, 285, and 504 keV). The excellent characterization of this band leaves little doubt about its identification with a $\frac{5}{2}[422]$ Nilsson state. This identification plays a pivotal role in the interpretation of the structure of the strongly deformed odd-A nuclei in the $A \simeq 100$ region. Confidence in the $5/2^+$ assignments to the ^{99}Y and ^{101}Y ground states is used to establish I^π values for other members of the isobaric chains and to determine (or at least limit) the

I^{π} values for many of the excited states. It has also been remarked[25] that the $5/2^+$ assignment to the ground state of ^{99}Y is the ultimate basis for spin assignments in the $N=59$ isotones.[24]

The two negative-parity bands associated with the $\frac{3}{2}[301]$ and $\frac{5}{2}[303]$ Nilsson states in both Y isotopes are also quite similar, once the reversal of the ordering of the bandheads is taken into account. (Assignments for these two bands are also made in ^{103}Nb,[17] but the data presented is insufficient to make a detailed comparison with the Y isotopes.) The similarity is best appreciated through consideration of the particle-rotor calculations discussed in Sec. III A. The reversal of the bandheads is reproduced by using a slightly smaller value of μ for ^{101}Y. Greater Coriolis mixing is deduced for ^{101}Y than for ^{99}Y, as expected with closer spacing of levels of like spin in ^{101}Y. The $M1$ parameter g' is 0.7 and the $\Delta K=0$ $E1$ parameter H is 2.7 for both nuclei. (All of the γ-ray parameters have an estimated accuracy of $\sim 10\%$.) However, the $E1$ parameter H for $\Delta K=\pm 1$ γ-rays differs significantly, being 0.9 for ^{99}Y and -0.3 for ^{101}Y. (Since the full γ-decay patterns also involve $M1$ transitions, the relative strength of $M1$ and $E1$ γ-rays determines the actual value of one of the two H factors, which we have chosen to be the H factor for $\Delta K=0$.) The ratio of H factors changes from $+3$ for ^{99}Y to -9 for ^{101}Y. The sign change cannot be avoided in reproducing the γ-decay patterns observed for the $\frac{3}{2}[301]$ and $\frac{5}{2}[303]$ bands in ^{101}Y. The reversal in the energy order of these bandheads in ^{101}Y from that in ^{99}Y causes a reversal in the sign of the admixed component in the wave functions of the bands. Combining the wave-function sign changes with the H-factor sign changes results in no change in the relative phases of the two pure-band contributions to the calculated $E1$ amplitudes for ^{101}Y and ^{99}Y. Thus the γ-decay patterns observed in both nuclei indicate relative phases that are somehow unaffected by the reversal in the energy order of the bands.

A possible explanation for the apparent sign change in H for $\Delta K=\pm 1$ is that it may be due instead to the pairing factor P^- that also multiplies each $E1$ matrix element. For both nuclei we used the BCS estimate $P^-=UU'-VV'$, as discussed in Ref. 7. With this estimate, the sign of P^- for either band is the same in both nuclei. Other estimates for P^- could result in a difference in its sign for ^{99}Y than for ^{101}Y for one of the two bands. As an example, allowing the BCS Fermi energy to be adjusted (rather than being fixed by the usual BCS particle-number constraint) could cause a change in both the sign and magnitude of P^-. If this were the case, then the signs of the deduced values of H would not change, although the values of H would be different from the values deduced with the highly constrained model described here.

Also of interest are other expected unique-parity bands, particularly the elusive band associated with the $\frac{3}{2}[431]$ Nilsson state. For ^{99}Y,[8] the levels at 1119 and 1213 keV were assigned as the first two levels of such a band. It now appears likely that this assignment is wrong. As can be seen in Fig. 11, the energy agreement with the particle-rotor calculation of Ref. 7 was good (especially since no bandhead adjustments were made in Ref. 7 as are done in the present calculations), but these two levels decay only to members of the negative-parity bands. The observed γ-decay pattern is quite different from that predicted by the model calculations, and an unusually large $E1$ enhancement factor H is required to explain[7] the observed γ-decay pattern if these levels are assigned to a $\frac{3}{2}[431]$ band. However, comparison with the results for ^{101}Y suggests that the 1119- and 1213-keV levels in ^{99}Y may instead be the $3/2^-$ and $5/2^-$ members of a $\frac{1}{2}[301]$ band, where the $1/2^-$ bandhead was unobserved in the experiment of Ref. 8. (A possible $1/2^-$ level was observed at 600 keV, but it is much too low in energy to be the $\frac{1}{2}[301]$ bandhead.) As noted in Sec. III, at the present time we cannot make an unambiguous assignment for the members of the $\frac{3}{2}[431]$ band in ^{101}Y. The $\frac{3}{2}[431]$ location now appears to be even more uncertain for ^{99}Y. On the other hand, we have a strong candidate in both ^{99}Y and ^{101}Y for a $\frac{1}{2}[431]$ band. Furthermore, the observed $\Delta K=2$ γ-rays from this band to the ground band indicate that a $\frac{3}{2}[431]$ band must be nearby in order to provide the necessary Coriolis mixing. Therefore, although the $\frac{3}{2}[431]$ bandhead is not yet located in either of these Y isotopes, the present data indicates that it should lie near (within a few hundred keV) the $\frac{1}{2}[431]$ bandhead.

It has been suggested[26] (on the basis of IBFM/PTQM calculations) that the $K=\frac{3}{2}$ band at 536 keV in ^{99}Y should be assigned as $\frac{3}{2}[431]$ rather than the $\frac{3}{2}[301]$ assignment of Refs. 7 and 8. However, unique-parity bands have highly constrained γ-decay properties. As was recently shown,[27] the purity of the wave functions for unique-parity orbitals and the validity of the dipole Alaga rules impose strong constraints on the choice of Nilsson orbital for a band. This choice can be far more crucial than the version of particle-rotor model or particular values for the model parameters. The assignment of $\frac{3}{2}[431]$ to the bandhead at 536 keV in ^{99}Y has been examined in Ref. 27, where it is shown that this assignment is incompatible with the observed γ-decay patterns. Since the band at 510 keV in ^{101}Y has similar properties, the arguments of Ref. 27 apply as well to ^{101}Y. The most telling point concerns the intensity ratio of low-energy intraband to higher-energy interband $M1$ γ-rays between unique-parity bands. Such ratios are constrained by Alaga rules and are quite small because of the energy-cubed factor. For example, if the 510-keV band in ^{101}Y were $\frac{3}{2}[431]$, then an intraband $M1$ γ-ray such as the 80-keV $\frac{5}{2}\rightarrow\frac{3}{2}$ or the 124-keV $\frac{7}{2}\rightarrow\frac{5}{2}$ γ-ray would be only $\sim 1\%$ of the intensity of an interband $M1$ γ-ray from the same level to the ground band. Since all observed intraband γ-rays have intensities that are ~ 100 times larger than permitted by the unique-parity constraints, a $\frac{3}{2}[431]$ assignment for the lowest $K=\frac{3}{2}$ band is incorrect for ^{101}Y as well as for ^{99}Y. The validity of such a unique-parity "rule" is empirically verified by deformed odd-A rare-earth and actinide nuclei. In all such nuclei with two unique-parity bands well separated in energy, no low-energy intraband γ-rays have intensities large enough to be observed,[28] as predicted by this unique-parity "rule."

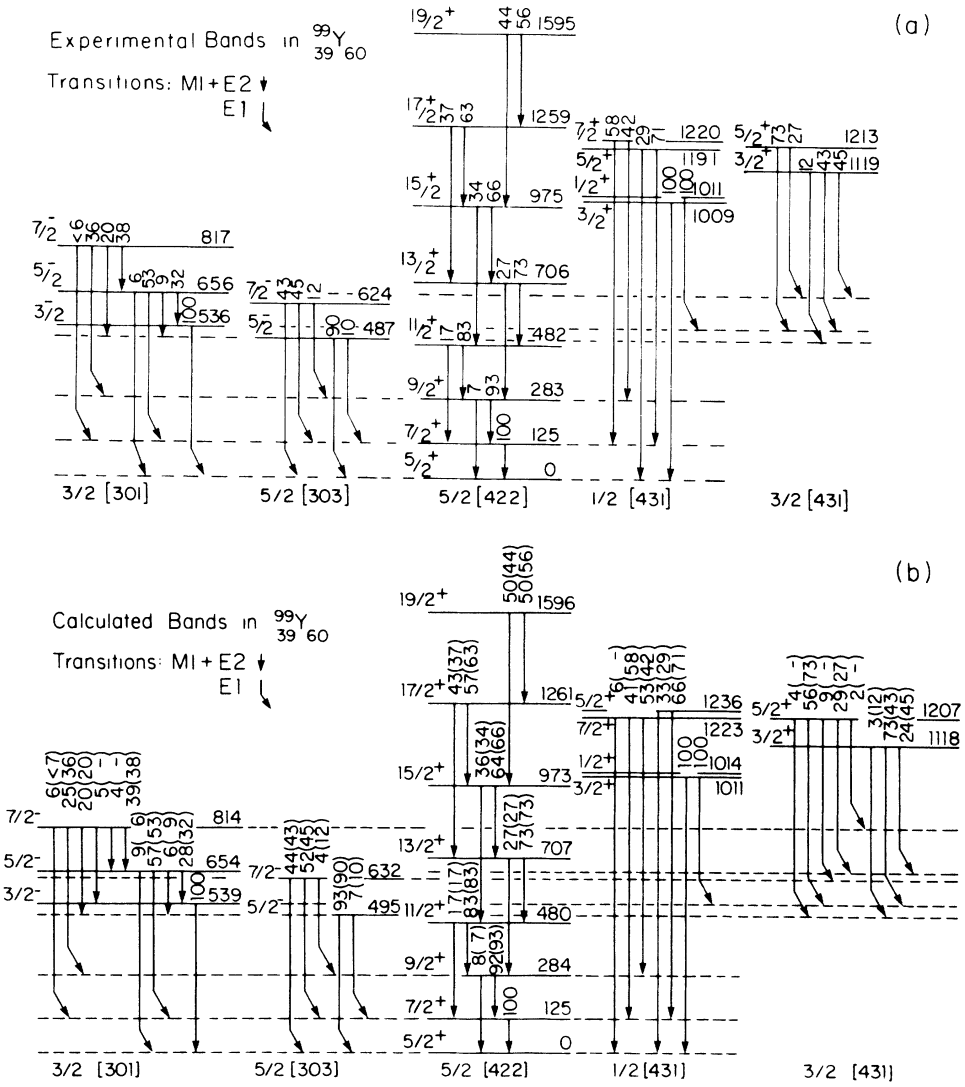

FIG. 11. Rotational bands and relative γ-ray intensities for levels in ^{99}Y. Experimental bands, (a), are from Ref. 8. One-quasiparticle bands, (b), were calculated (Ref. 7) from a particle-rotor model with Coriolis coupling. For comparison, experimental γ-ray intensities are also given, (b), in parentheses.

TABLE V. Lifetimes of bandheads that decay by $E1$ γ-rays.

	Bandhead	Energy (in keV)	Bandhead half-life (in ns) Calculated[a]	Experimental[b]
^{99}Y	$\frac{5}{2}$[303]	487	0.02	
	$\frac{3}{2}$[301]	536	0.04	
	$\frac{1}{2}$[431]	1011	0.08	
^{101}Y	$\frac{5}{2}$[303]	666	0.02	
	$\frac{3}{2}$[301]	511	0.46	
	$\frac{1}{2}$[431]	1217	0.02	
^{103}Nb	$\frac{5}{2}$[303]	164	4.8	4.7±0.5
	$\frac{3}{2}$[301]	248	1.9	2.0±0.6
	$\frac{1}{2}$[431]			

[a]See text for discussion of H values used in calculations.
[b]Reference 17.

Calculated half-lives of the bandheads that decay by $E1$ γ-rays for the nuclei ^{99}Y, ^{101}Y, and ^{103}Nb are shown in Table V. Experimental values[17] exist only for ^{103}Nb. As is discussed in Ref. 7, there are three important factors in calculating these $E1$ half-lives: the cube of the γ-ray energy, the square of the pairing factor P^-, and the square of the amplitude factor $GE1(K \rightarrow K')$. For a given K and K', the $GE1$ factors are essentially identical for all three nuclei in Table V. The half-lives shown for ^{99}Y and ^{103}Nb have been deduced from the calculation of Ref. 7 (i.e., $H=1.0$ for $\Delta K=\pm 1$ and $H=3.0$ for the $\Delta K=0$). As discussed in Ref. 7, the differences in calculated level lifetimes for ^{99}Y and ^{103}Nb are due mainly to the energy-cubed and pairing factors. The H values of the present work are used for ^{101}Y. Its H value of -0.3 for $\Delta K=\pm 1$ is the reason why the calculated half-life for the $\frac{3}{2}[301]$ bandhead is significantly longer than for ^{99}Y. Although the shorter-level lifetimes expected for ^{99}Y and ^{101}Y would be more difficult to measure than the few ns lifetimes in ^{103}Nb, the Y lifetimes are very important data since they would provide direct determinations of the product HP^- for each band. Comparison of these values with the indirectly determined HP^- values of the present study would provide a critical test of our knowledge of the single-particle Nilsson states associated with the low-lying bands.

In conclusion, the simple particle-rotor model calculations are able to reproduce the observed band structures of both ^{101}Y and ^{99}Y. The parameters of the model are, for the most part, similar for both nuclei. A few of the parameters, however, appear to be significantly different. Whether these parameter differences are due to actual structural changes in the two isotopes or reflect instead inadequacies in the model is unclear at present. Certain additional studies of these nuclei are suggested, such as a restudy of ^{99}Y in order to identify members of $\frac{1}{2}[301]$ and $\frac{3}{2}[431]$ bands. Level lifetime measurements would also be very useful, since they would provide additional constraints on the deduced values of the γ-ray parameters Q_0, g', H, and the pairing factor P^-. Comprehensive studies of rotational bands in other deformed odd-Z $A \sim 100$ nuclei, particularly ^{101}Nb and ^{103}Nb, should also provide important information to further our understanding of this exotic nuclear region.

ACKNOWLEDGMENTS

The authors wish to express their appreciation to the neutron nuclear physics group at BNL and the TRISTAN staff for their excellent technical support and for their interest in this work. Two of the authors (FKW and JCH) acknowledge the assistance in data analysis by C. M. Hanson and R. R. Holmes. This work was supported by the U.S. Department of Energy under Contract Nos. DE-AS05-79ER10495, W-7405-eng-82, and DE-AC07-76CH00016.

*Permanent address: Institute for Nuclear Studies, Warsaw, Poland.

[1]F. K. Wohn, J. C. Hill, C. B. Howard, K. Sistemich, R. F. Petry, R. L. Gill, H. Mach, and A. Piotrowski, Phys. Rev. C **33**, 677 (1986).

[2]L. K. Peker, F. K. Wohn, J. C. Hill, and R. F. Petry, Phys. Lett. **169B**, 323 (1986).

[3]P. Federman and S. Pittel, Phys. Rev. C **20**, 820 (1979).

[4]G. Gneuss and W. Greiner, Nucl. Phys. **A171**, 449 (1971).

[5]P. Tondeur, Nucl. Phys. **A359**, 278 (1981).

[6]M. E. Bunker and C. W. Reich, Rev. Mod. Phys. **43**, 348 (1971).

[7]F. K. Wohn, J. C. Hill, and R. F. Petry, Phys. Rev. C **31**, 634 (1985).

[8]R. F. Petry, H. Dejbakhsh, J. C. Hill, F. K. Wohn, M. Shmid, and R. L. Gill, Phys. Rev. C **31**, 621 (1985).

[9]E. Monnand, J. A. Pinston, F. Schussler, B. Pfeiffer, H. Lawin, G. Battistuzzi, K. Shizuma, and K. Sistemich, Z. Phys. A **306**, 183 (1982).

[10]R. A. Meyer, E. Monnand, J. A. Pinston, F. Schussler, I. Ragnarsson, B. Pfeiffer, H. Lawin, G. Lhersonneau, T. Seo, and K. Sistemich, Nucl. Phys. **A439**, 510 (1985).

[11]M. Shmid, R. L. Gill, and C. Chung, Nucl. Instrum. Methods **211**, 287 (1983).

[12]F. K. Wohn, J. C. Hill, R. F. Petry, H. Dejbakhsh, Z. Berant, and R. L. Gill, Phys. Rev. Lett. **51**, 873 (1983).

[13]P. Möller and J. R. Nix, At. Data Nucl. Data Tables **26**, 165 (1981).

[14]*Table of Isotopes*, 7th ed., edited by C. M. Lederer and V. S. Shirley (Wiley, New York, 1978), p. 437.

[15]B. Pfeiffer, E. Monnand, J. A. Pinston, J. Münzel, P. Möller, J. Krumlinde, W. Ziegert, and K.-L. Kratz, Z. Phys. A **317**, 123 (1984).

[16]K. Shizuma, H. Ahrens, J. P. Bocquet, N. Kaffrell, B. D. Kern, H. Lawin, R. A. Meyer, K. Sistemich, G. Tittel, and N. Trautmann, Z. Phys. A **315**, 65 (1984).

[17]T. Seo, A. M. Schmitt, H. Ahrens, J. P. Bocquet, N. Kaffrell, H. Lawin, G. Lhersonneau, R. A. Meyer, K. Shizuma, K. Sistemich, G. Tittel, and N. Trautmann, Z. Phys. A **315**, 251 (1984).

[18]J. Fujita, G. T. Emery, and Y. Futami, Phys. Rev. C **1**, 1060 (1970).

[19]M. Epherre, G. Audi, C. Thibault, R. Klapisch, G. Huber, F. Touchard, and H. Wollnik, Phys. Rev. C **19**, 1504 (1979).

[20]K. Kumar, B. Remaud, P. Aguer, J. S. Vaagen, A. C. Rester, R. Foucher, and J. H. Hamilton, Phys. Rev. C **16**, 1235 (1977).

[21]W. Ogle, S. Wahlborn, R. Piepenbring, and S. Fredriksson, Rev. Mod. Phys. **43**, 424 (1971).

[22]R. Popli, J. A. Grau, S. I. Popli, L. E. Samuelson, F. A. Rickey, and P. C. Simms, Phys. Rev. C **20**, 1350 (1979). [See also H. A. Smith and F. A. Rickey, Phys. Rev. C **14**, 1946 (1976) and S. Zeghib, F. A. Rickey, and P. C. Simms, Phys. Rev. C **34**, 1451 (1987).]

[23]I. Ragnarsson, in *Proceedings of the International Conference on the Properties of Nuclei Far from Stability*, Leysin, Switzerland, 1970, CERN Report No. 70-30,847, 1970 (unpublished).

[24]R. A. Meyer, Hyperfine Interactions **22**, 385 (1985).

[25]F. Buchinger, E. B. Pamsey, R. E. Silverans, P. Lievens, E. Arnold, W. Neu, R. Neugert, K. Wendt, G. Ulm, and the ISOLDE Collaboration, Z. Phys. A **327**, 361 (1987).

[26]B. Pfeiffer, S. Brant, K.-L. Kratz, R. A. Meyer, and V. Paar, Z. Phys. A **325**, 487 (1986).

[27]F. K. Wohn, Phys. Rev. C **36**, 1204 (1987).

[28]*Table of Isotopes*, 7th ed., edited by C. M. Lederer and V. S. Shirley (Wiley, New York, 1978).